Received: 26 July 2022 | Revised: 6 January 2023 | Accepted: 25 January 2023

DOI: 10.4218/etrij.2022-0242

ORIGINAL ARTICLE

ETRI Journal WILEY

Activity recognition of stroke-affected people using wearable sensor

Anusha David[1] | Rajavel Ramadoss[1] | Amutha Ramachandran[1] | Shoba Sivapatham[2]

[1]ECE Department, SSN College of Engineering, Kalavakkam, Chennai, Tamil Nadu, India

[2]Center for Advanced Data Science (CADS), Vellore Institute of Technology, Chennai Campus, Chennai, Tamil Nadu, India

Correspondence
Shoba Sivapatham, Center for Advanced Data Science (CADS), Vellore Institute of Technology, Chennai Campus, Chennai, Tamil Nadu, India.
Email: shoba.s@vit.ac.in

Abstract

Stroke is one of the leading causes of long-term disability worldwide, placing huge burdens on individuals and society. Further, automatic human activity recognition is a challenging task that is vital to the future of healthcare and physical therapy. Using a baseline long short-term memory recurrent neural network, this study provides a novel dataset of stretching, upward stretching, flinging motions, hand-to-mouth movements, swiping gestures, and pouring motions for improved model training and testing of stroke-affected patients. A MATLAB application is used to output textual and audible prediction results. A wearable sensor with a triaxial accelerometer is used to collect preprocessed real-time data. The model is trained with features extracted from the actual patient to recognize new actions, and the recognition accuracy provided by multiple datasets is compared based on the same baseline model. When training and testing using the new dataset, the baseline model shows recognition accuracy that is 11% higher than the Activity Daily Living dataset, 22% higher than the Activity Recognition Single Chest-Mounted Accelerometer dataset, and 10% higher than another real-world dataset.

KEYWORDS

accelerometer, human activity, LSTM, recognition, strokes, wearable sensor

1 | INTRODUCTION

Sensor-based human activity recognition (HAR) is a challenging and important form of healthcare assistance for the elderly and physically/mentally disabled people who wish to live independently in their homes, as opposed to in an institutional care facility. Researchers have used several types of wearable sensors to capture and recognize HAR data, and some of the most widely used sensors include triaxial accelerometers and gyroscopes. With these, researchers have employed a variety of algorithmic methods to interpret the data. Recently, deep-learning algorithms [1, 2] have been employed for this purpose, showing very promising performance. Such approaches [3] combine shallow and learned features taken from an inertial sensor for time-series data classification. Another study [3] addressed some of the problems with deep learning frameworks when on-node computation was required, and a semisupervised deep temporal long short-term memory (LSTM) ensemble method was proposed [4] for HAR using smartphone inertial sensors. This method provided significant improvements over other semisupervised techniques that rely on various proportions of labeled training data.

Smartphone-based convolutional neural networks (CNNs) have been proposed for HAR [5], and to boost their accuracy, CNN-based ensemble models have incorporated local dependencies and scale-invariant aspects of sensor time-series data, resulting in a very high 96.11 % recognition accuracy. Another study [6] proposed a HAR method that uses data obtained from a single triaxial accelerometer. The model transforms the accelerometer data into square acceleration images. An overview of HAR methods using smartphone inertial sensor data was presented in [7], and the model of [8] provided an efficient CNN-based HAR method that uses an encoding technique to transform inertial sensor inputs into a different picture format. Those authors compared their model performances using their own datasets and other public datasets. A novel approach was proposed in [9] that operates in unconstrained HAR environments (e.g., Apple TV, Apple Watch, Apple Remote, and iPhone), demonstrating how a CNN with discrete cosine transform) as a feature improves accuracy in HAR. The researchers of [10] presented a new CNN-based HAR model that used signals from magnetometers, accelerometers, and gyroscopes embedded in smartphones. Relatedly, accurate HAR detection was achieved by integrating photoplethysmography and triaxial accelerometer signals, achieving an accuracy of 95% with less memory and computational power burdens than other models [11]. The cost, power, and complexity of HAR devices were reduced by using low-cost recurrent neural networks (RNNs) that interfaced with embedded cloud-based microcontrollers for processing. The related model provided an accuracy of 90.50% with less overall time and resources [12].

A CNN-based ensemble approach was proposed to resolve the uncertainty between various HAR activities, achieving an accuracy of 96.29.

All of the above-mentioned studies focused mainly on the recognition of common activities, neglecting special behaviors. In this direction, Bensalah and others developed an upper-limb assessment system specifically for stroke-affected patients using data collected from digital watches. Their assessment system automatically detects and recognizes a variety of constrained activities [13]. Braakhuis and others developed a day-to-day activity stroke monitoring system for routine physical therapy. A therapist-based survey indicated that the system was the most useful among the available tools, but this monitoring system was used by only 27% of the patients. Hence, proper education of its usage and benefits were found to lead to more efficient monitoring of stroke affected people's activities [14].

A general HAR system architecture using wearable sensors is presented in Figure 1 based on extant studies. The present study takes a different approach to dataset construction by considering the recognition of special

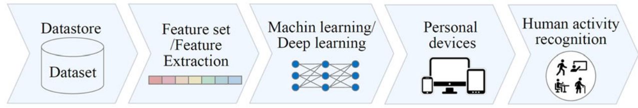

FIGURE 1 General human activity recognition architecture for wearable device data collection.

activities, such as forward stretching, upward stretching, flinging motions, hand-to-mouth actions, swiping gestures, and pouring. Because a stroke-victim activity dataset of this nature is unavailable to the public, this work provided one with the support of student volunteers. A real-time HAR system was built using a standard LSTM-RNN baseline, and MATLAB was used to produce an application that converts the model output to textual and audible formats, which can be used to directly assist caretakers to fulfill their needs in time. Model performance based on training and testing with our new dataset was compared with those of other publicly available datasets, and the proposed system with its dataset showed the highest recognition accuracy. Detailed comparisons are provided in the Results and Discussion sections.

The rest of this study is constructed as follows. Section 2 examines a few other HAR datasets. The LSTM-RNN model and its components are described in Section 3. This is followed by Section 4, which presents an evaluation of the performance, and Section 5 presents conclusions and future research recommendations.

2 | REVIEW OF EXTANT HAR DATASETS

Various HAR datasets are available freely to researchers. Table 1 highlights some of these with additional details, such as the number of participants, activities, sensor used, and the location of the sensor. The activities of daily living (ADL) dataset [15] provides labeled recordings of simple human activities, and the data were collected using a wrist-placed accelerometer mainly targeting the recognition of common daily activities.

The Activity Recognition from a Single Chest-Mounted Accelerometer (ARSC-MA) dataset [16] supports the identification and verification of persons based on their mobility patterns. A wearable accelerometer sensor is placed on the chest, and stair-climbing, standing, talking, walking, and working activities are predicted. A real-world dataset was developed to support this real-time HAR tool using mobile-device sensors [17]. A triaxial accelerometer sensor is placed on the waist for data collection, and raw data are transformed into monochrome and colored images [18]. A stroke-patient dataset created by the researcher in [19] contains healthy and stroke HAR data from 17 patients. Another dataset was created by [20] from

TABLE 1 Commonly used human activity recognition (HAR) datasets.

Dataset	Age group	Sampling frequency	No. of persons	Activities	Sensor	Sensor locations
Activities of Daily Living (ADL) dataset [15]	65–85 years	20 Hz	16	Climb stairs, Drink glass, Get up bed, Pour water, Sit down chair, Stand up chair	Triaxial accelerometer	Attached to right wrist
Single Chest-Mounted Accelerometer (ARSC-MA) dataset [14]	Not mentioned	50 HZ	15	Working at computer, Standing up, Walking and going, updown stairs, Standing, Walking, Going upDown stairs, Walking and talking with someone, Talking while standing	Triaxial accelerometer	Wearable accelerometer mounted on the chest
Real-world dataset [16]	30–50 years	50 HZ	15	Climbing up, Climbing down, Jumping, Lying, Sitting, Standing, Walking	Triaxial accelerometer	Accelerometer mounted on waist
Center for Machine Learning and Intelligent Systems (UCI) HAR dataset [18]	19–48 years	50 Hz	30	Walking, Walking upstairs, Walking downstairs, Sitting, Standing, Laying	Triaxial accelerometer	Wearing a smartphone (Samsung Galaxy S II) on the waist. Using its embedded accelerometer

home and laboratory experiments reflecting specific gait improvements in stroke patients and healthy patients for various activities of HAR.

The Center for Machine Learning and Intelligent Systems (UCI) HAR dataset is the most popular [21] and contains preprocessed sensor input and feature vectors obtained from the time-frequency domain. This dataset was developed to recognize human activities in [21] using triaxial accelerometer smartphone data.

The datasets highlighted thus far focus mainly on common activities, which may not be suitable for actual stroke-patient monitoring. Hence, in this study, a new dataset using triaxial accelerometer data is provided. The details, including the actions and recording environments, are discussed in the following section.

3 | PROPOSED REAL-TIME HAR DATASET

The proposed dataset as applied to the baseline LSTM-RNN is illustrated in Figure 2. Activities such as forward stretching, upward stretching, flinging, hand-to-mouth movements, swiping, and pouring are covered. Using the additional MATLAB application, the recognized activities are displayed in real time as textual and audible outputs. The following subsection explains the data collection, feature extraction, and network training and testing.

3.1 | Data acquisition and preprocessing

Because this work is a special case that focuses on stroke-affected patients HAR, the dataset was collected by the authors using a Shimmer-brand sensor that provides wireless connectivity [22]. The Shimmer brand offers comprehensive wearable sensor solutions for medical, neurological, and clinical research industries using wearable inertial measurement embedded devices that include accelerometers, gyroscopes, and magnetometers. Real-time kinematic data were captured from the sensors, and the gathered data were broadcast to a Bluetooth-enabled data collection device.

In this study, 28 healthy persons (18 males and 20 females) participated, and their data are summarized in Table 2. The individuals wore an accelerometer sensor (AS) while performing the prescribed tasks. The AS is a device that measures the force of acceleration. The acquired data were transmitted via Bluetooth to a laptop running Windows 10 with preinstalled Consensys Pro software. The participants, who were trained to perform six specific actions, were seated comfortably in chairs

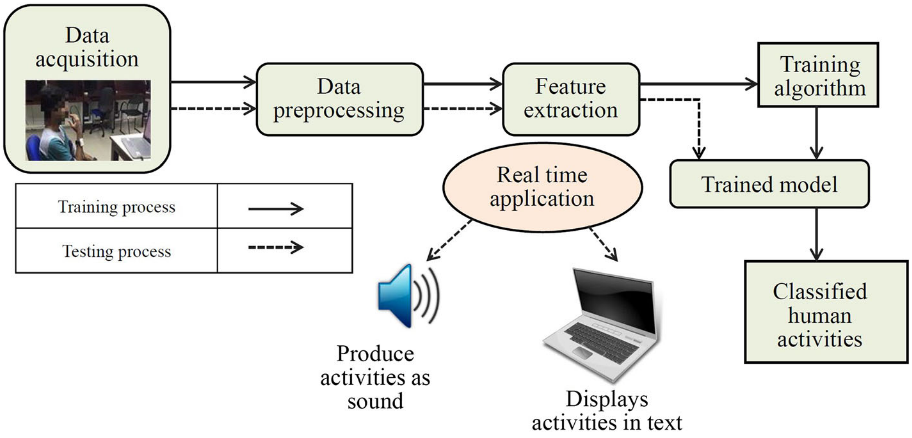

FIGURE 2 Proposed human activity recognition system.

TABLE 2 Details of participants in the dataset compilation.

Total persons	Males	Females	Age (avg)	Weight (avg)	Height (avg)
38	18	20	24 (years)	65 (kg)	5.3 (ft)

FIGURE 3 Sample image (photo) of a person performing the six actions.

facing a computer. Each participant was required to repeat each action 10 times. The details and a sample photo are shown in Figure 3. The collected sensor data were preprocessed for feature extraction.

- Action 1—Forward stretch: The person stretches his/her forearm in a forward direction.
- Action 2—Upward stretch: The person stretches his/her hand in an upward direction
- Action 3—Fling: The person pretends to throw a virtual object in a forward direction
- Action 4—Hand-to-mouth: The person brings his/her arm near to the mouth and returns it to its initial position.
- Action 5—Swipe: The person stretches his/her hand and swipes in the clockwise direction.
- Action 6—Pouring: The person pretends to clutch a virtual object and pours by rotating the wrist.

3.2 | Feature extraction

Reliable features are crucial to classification tasks [23], and some researchers have used raw signals directly for this purpose. However, raw signals are not viable for compiling larger datasets. In this study, reliable features were retrieved from the raw acceleration data first, and used for model training to speed-up the process and improve recognition accuracy. The following 20 features were extracted:

1. Mean (μ): The arithmetic mean (average) of a set of numbers.

$$\mu = \frac{1}{n}\sum_{i=1}^{n} x_i. \tag{1}$$

2. Standard deviation (σ): The amount of deviation of values or average mean data,

$$\sigma = \sqrt{\frac{1}{n}\sum_{i=1}^{n}(x_i-\mu)^2}. \tag{2}$$

3. Index of dispersion (D): The ratio of variance to mean,

$$D = \frac{\sigma^2}{\mu}. \tag{3}$$

4. Absolute difference (A): The measure of absolute difference between two variables,

$$A = |x-y| \geq 0. \tag{4}$$

5. Maximum peak amplitude (P): The amplitude of a wave at its greatest magnitude of deflection,

$$P = A\sin(2*\pi*f*t). \tag{5}$$

6. Information entropy (E): The negative logarithm of the probability mass function of the value (for each possible data value),

$$E = \sum_{i=1}^{n} p_i \log_2\left(\frac{1}{pi}\right). \tag{6}$$

7. Skewness (S): The asymmetry of a real-valued random variable's probability distribution around its mean,

$$S = \sum_{i=1}^{n} \frac{\frac{(x_i-\mu)^3}{n}}{\sigma^3}. \tag{7}$$

8. Kurtosis (K): The determinant of whether data are heavy- or light-tailed compared with a normal distribution,

$$K = \sum_{i=1}^{n} \frac{\frac{(x_i-\mu)^4}{n}}{\sigma^4}. \tag{8}$$

9. Root mean square (RMS): The square root of the of the squares of a group of values,

$$\mathrm{RMS} = \sqrt{\frac{\sum_{i=1}^{n} x_i^2}{n}}. \tag{9}$$

10. Amplitude (y): The displacement of a particle of a medium (represented by A).

$$A = \sin(\omega t + \phi) \tag{10}$$

11. Median absolute (MA): The variability of a univariate sample of quantitative data,

$$\mathrm{MA} = \sum_{i=1}^{n} \left|\frac{x_i - \mu}{n}\right|. \tag{11}$$

12. Cross-correlation coefficient (r): The similarity of two series as a function of the distance between each value,

$$r = \frac{n\left(\sum_{i=1}^{n} xy\right) - \left(\sum_{i=1}^{n} x\right)\left(\sum_{i=1}^{n} y\right)}{\sqrt{\left[n\sum_{i=1}^{n} x^2 - \left(\sum_{i=1}^{n} x^2\right)\right]\left[n\sum_{i=1}^{n} y^2 - \left(\sum_{i=1}^{n} y^2\right)\right]}}. \tag{12}$$

13. Mean absolute deviation (MAD): The average distance between each data point and the mean,

$$\mathrm{MAD} = \sum_{i=1}^{n} \left|\frac{x_i - \bar{x}}{x}\right|. \tag{13}$$

14. Covariance (cov): The measure of two random variables' combined variability,

$$\mathrm{cov} = \sum_{i=1}^{n} \frac{(x_i - \overline{x})}{n}. \tag{14}$$

15. Variance (σ^2): The expectation of a random variable's squared variation from its mean,

$$\sigma^2 = \sum_{i=1}^{n} \frac{(x^2 - \mu^2)}{n}. \tag{15}$$

16. Band power (BP): The typical power within a frequency range, specified as a two-element vector,

$$\mathrm{BP} = \cos(2 \times \pi \times 100 \times x_i). \tag{16}$$

17. Cross-correlation (rk): The relationship between measures with the same maximum and minimum values in different time-series,

$$\mathrm{rk} = \sum_{i=1}^{n} \frac{(x_i - \overline{x})}{(x_i - \overline{x})^2}. \tag{17}$$

18. Interquartile range (IQR): The variation between the upper and lower quartile values in a collection of data,

$$\mathrm{IQR} = \left(\frac{3(n+1)}{4}\right) - \left(\frac{n+1}{4}\right). \tag{18}$$

19. Norm (N): The sum of the squares of a complex number's real and imaginary components, or the positive square root of this sum, providing the product of a complex number and its conjugate,

$$N = \sqrt{\sum_{i=1}^{n} |a_i^2|}. \tag{19}$$

20. Median: The value that separates the data's upper and lower halves,

$$\mathrm{Median} = \left(\frac{n+1}{4}\right)^{\mathrm{th}} \mathrm{term}. \tag{20}$$

3.2.1 | LSTM-RNN classifier

An RNN is a generalized version of a feed-forward neural network with indoor memory. The advantage of an RNN

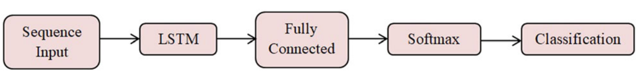

FIGURE 4 Architecture of a simple recurrent neural network for classification.

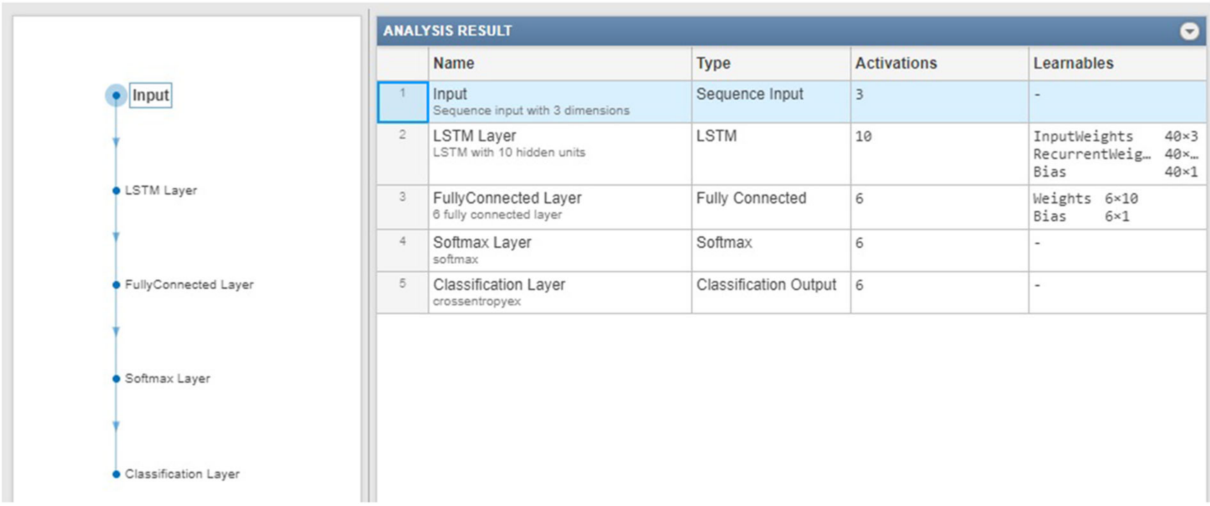

FIGURE 5 Designed long short-term memory network for human activity recognition.

TABLE 3 Hyperparameters used to fine-tune the long short-term memory recurrent neural network model.

Parameters	Range
Number of input nodes	240 × 6
Number features	20
Hidden units	1000
Batch size	64
Number of output nodes	240 × 1
Activation (hidden)	Rectified linear unit
Activation (output)	SoftMax
MaxEpochs	100
Learning method	Adam
Learning rate	0.001
Dropout rate	0.2
Classes	6
Validation data	10%
Cost function	Mean squared error

is that it can model time series data such that each sample is assumed to be dependent. The LSTM network is an augmented RNN that simplifies past data recall. Hence, it is well-suited for classifying and predicting statistics when there are time lags of unknown durations [24].

This study used the LSTM network to train and classify the designated actions of stroke-affected patients. The baseline LSTM-RNN network architecture is shown in Figure 4, in which the sequence input layer precedes the LSTM layer. To forecast the class label activities, the network includes a fully connected layer, a SoftMax layer, and an output layer. The LSTM-RNN was designed using MATLAB to recognize the activities, as shown in Figure 5. The extracted features are fed into the sequence input layer of the LSTM, which has 1000 hidden units to process the input feature sequence using a backpropagation algorithm. The detailed hyperparameters are shown in Table 3. Finally, to provide the final HAR output, the fully connected layer with the SoftMax activation function classifies the processed feature sequence into label classes.

4 | EXPERIMENTAL RESULTS AND DISCUSSIONS

The experimental outcomes of the proposed stroke-affected HAR model are presented in this section based on the prepared dataset comprising the six chosen activities of stroke-affected patients. The dataset was acquired from 38 participants (18 male and 20 female) who wore wearable accelerometer sensors on their right wrists. A total of 2280 samples were recorded, There were 10 samples for each activity. From all samples, 1824 (80%) were used for training, and 456 (20%) were used for testing. The proposed and compared model configurations were evaluated using precision, recall, accuracy, and F_1 score.

Precision is the ratio of the number of correct positive correct (P_c) to the total number of positive correct (P_c) and positive incorrect (P_{I_c}) estimates. The overall accuracy of the precision measure is classified as a positive estimate,

$$\text{Precision} = \frac{\text{Positive correct }(P_c)}{(\text{Positive correct }(P_c) + \text{Positive incorrect }(P_{I_c}))}. \tag{21}$$

Recall is the ratio of the number of positive correct guesses (P_c) to the total number of positive correct (P_c) and negative incorrect (N_{I_c}) guesses. An increase in the recall value indicates a more positive estimate,

$$\text{Recall} = \frac{\text{Positive correcta } (P_c)}{(\text{Positive correct } (P_c) + \text{Negative incorrect } (N_{I_c}))}. \tag{22}$$

The F_1 score is a single metric that combines precision and recall (harmonic mean),

$$F_1 \text{ Score} = \frac{2 * (\text{Precision} \times \text{Recall})}{(\text{Precision} + \text{Recall})}. \tag{23}$$

Accuracy reflects the performance across all classes, which is beneficial when all classes are equally essential.

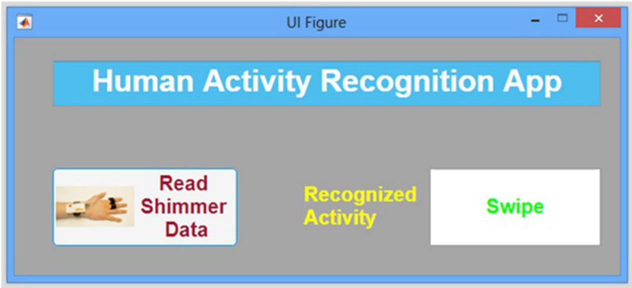

FIGURE 6 Proposed stroke-affected human activity recognition model.

TABLE 4 Recognition accuracy of our model with our prepared dataset compared with the same model with other datasets.

Data sets	Classification algorithm	Training accuracy	Testing accuracy
ADL [13]	RNN - LSTM	93%	78%
ARSC-MA [14]	RNN - LSTM	94%	67%
Real-world [15]	RNN - LSTM	98%	79%
Proposed	RNN - LSTM	100%	89%

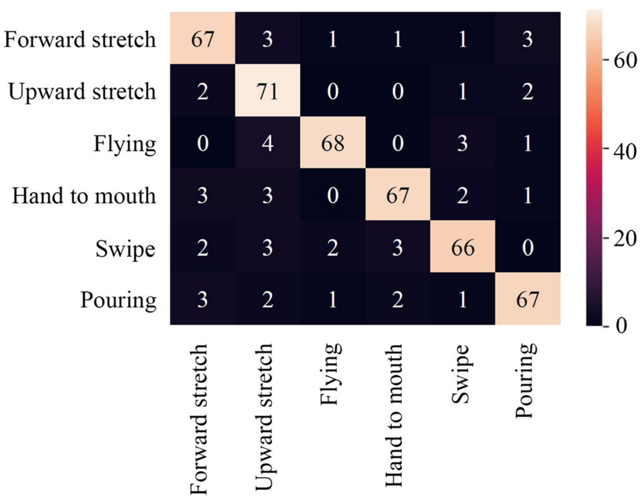

FIGURE 7 Performance confusion matrix for the long short-term memory recurrent neural network model based on training and testing with different datasets.

It is defined as the ratio of the total number of samples, $P_c + N_c + P_{I_c} + N_{I_c}$, to the sum of the number of correct positive guesses (P_c) and incorrect positive guesses (N_c),

$$\text{Accuracy} = \frac{P_c + N_c}{P_c + N_c + P_{I_c} + N_{I_c}}. \tag{24}$$

The proposed model is illustrated in Figure 6. All 456 testing samples were tested individually to measure

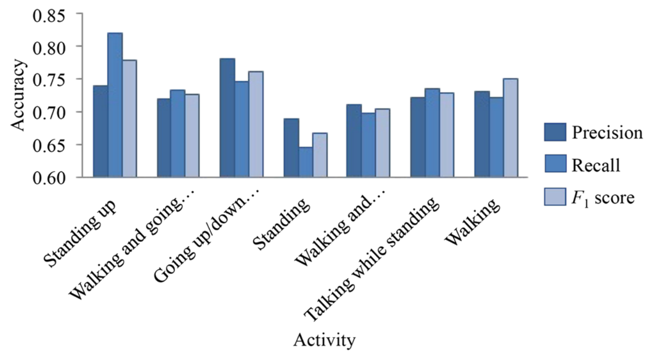

FIGURE 8 Score comparisons of the proposed long short-term memory recurrent neural network model trained and tested with the ARSC-MA dataset.

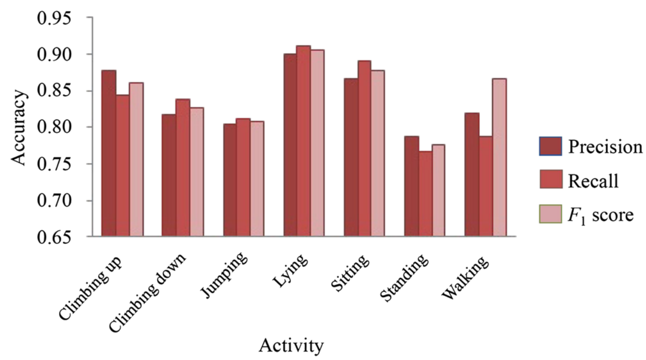

FIGURE 9 Score comparisons of the proposed long short-term memory recurrent neural network model trained and tested with the ADL dataset.

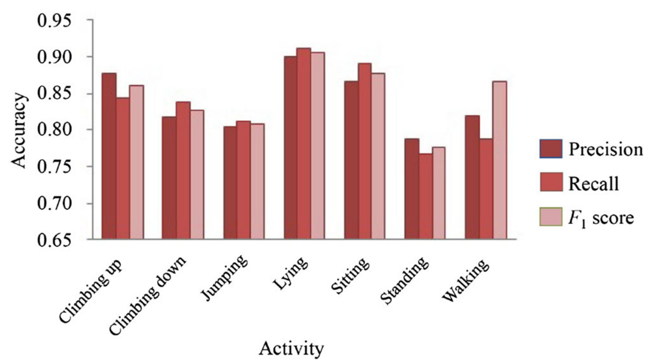

FIGURE 10 Score comparisons of the proposed long short-term memory recurrent neural network model trained and tested with the real-world dataset.

recognition accuracy (see Table 4). Using the proposed dataset, the model provided a recognition accuracy of 89%, which is greater than that of other datasets. A confusion matrix is displayed in Figure 7, where it can be seen that, apart from the upward stretching motion, all other classes had nearly equal classification accuracies of 88%. The upward stretch motion achieved a maximum classification accuracy of 93.14%. The same trend was observed in precision, recall, and F_1 score (see Figures 8–11 and Table 5).

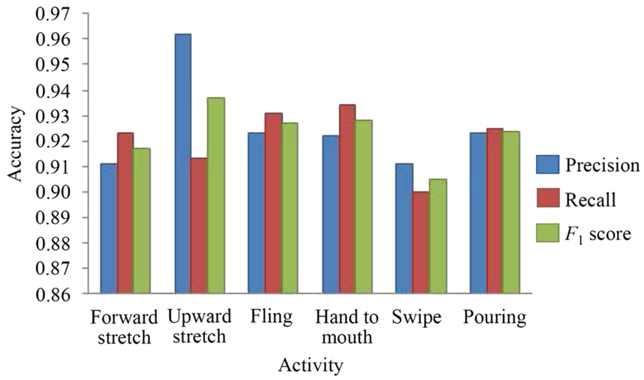

FIGURE 11 Score comparisons of the proposed long short-term memory recurrent neural network trained and tested with the proposed dataset.

Table 4 shows that the proposed system configuration using the prepared dataset improved recognition accuracy by 11% over the ADL dataset, 22% over the ARSC-MA dataset, and 10% over the real-world dataset. From the observations listed in Table 5, the precision, recall, and F_1 results of the proposed configuration with the prepared dataset were the best.

The baseline model was trained and tested using the ARSC-MA dataset focusing on the activities as shown in Figure 8. The real-time recognition accuracy was 67%, which was much lower than that of the model when tested and trained using the proposed dataset. The precision, recall, and F_1 scores for ARSC-MA were 19%–20% lower. t

The baseline model was trained and tested using the ADL dataset focusing on the activities shown in Figure 8. The real-time recognition accuracy was 78%, which is nearly 11% lower than that of the model when tested and trained using the proposed dataset. The precision, recall, and F_1 scores for ADL were 7%–8% lower, as shown in Figure 9. Finally, the model was trained and tested using the real-world dataset focusing on the activities shown in Figure 10. The real-time recognition accuracy was 79%, which is nearly 10% lower than that of the model when tested and trained using the proposed dataset. The

TABLE 5 Performance measures of different datasets and their respectively compared activities.

	ADL				ARSC-MA		
Activity	**Precision**	**Recall**	**F_1 score**	**Activity**	**Precision**	**Recall**	**F_1 score**
Climb stairs	0.830	0.790	0.810	Standing up	0.740	0.820	0.778
Drink glass	0.920	0.890	0.905	Walking and Going up Down stairs	0.720	0.734	0.727
Get up bed	0.880	0.850	0.865	Going up Down stairs	0.780	0.745	0.762
Stand up chair	0.780	0.800	0.790	Standing	0.690	0.645	0.667
Sit down chair	0.810	0.780	0.795	Walking and talking with someone	0.711	0.698	0.704
Pouring water	0.870	0.890	0.880	Talking while standing	0.722	0.735	0.728
				Walking	0.73	0.722	0.75

TABLE 5 (Continued)

		Real-world				Proposed		
Activity	**Activity**	**Precision**	**Recall**	**F_1 score**	**Activity**	**Precision**	**Recall**	**F_1 score**
Climb stairs	Climbing up	0.877	0.843	0.860	Forward stretch	0.911	0.923	0.917
Drink glass	Climbing down	0.817	0.837	0.827	Upward stretch	0.962	0.913	0.937
Get up bed	Jumping	0.804	0.812	0.808	Fling	0.923	0.931	0.927
Stand up chair	Lying	0.900	0.911	0.905	Hand to mouth	0.922	0.934	0.928
Sit down chair	Sitting	0.866	0.890	0.878	Swipe	0.911	0.900	0.905
Pouring water	Standing	0.788	0.766	0.777	Pouring	0.923	0.925	0.924
	Walking	0.820	0.788	0.866				

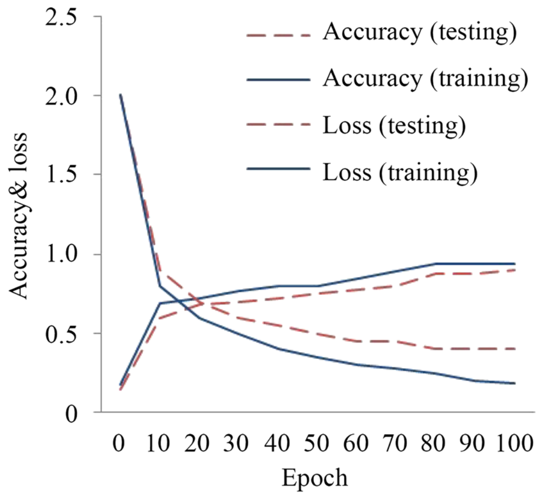

FIGURE 12 Accuracy and loss of the proposed long short-term memory recurrent neural network model based on the six simulated activities of the proposed dataset.

precision, recall, and F_1 scores for the real-world dataset were 13%–18% lower, as shown in Figure 11.

As shown in Figure 12, the classification accuracy of the baseline model when trained using the specially designed dataset was 89.11% after 100 epochs, which is significantly better than the classification accuracies from the other datasets. Notably, the activities and devices used to prepare all datasets differed. Therefore, strictly comparing the performance may not be fair and meaningful. Hence, we used several metrics, as shown in the figures and tables above.

5 | CONCLUSIONS

A new dataset to be used for the real-time activity recognition of stroke-affected patients was provided in this study. The six frequent recognition activities covered by the dataset included forward stretching, upward stretching, flinging, hand-to-mouth, swiping, and pouring. The new dataset comprises data collected using a Shimmer-brand device equipped with an accelerometer. The dataset was preprocessed, and 20 common features were extracted. A standard LSTM-RNN was trained and tested to recognize activities in real time. The recognized activities were provided as text and sound output using a specially designed MATLAB application that we provided. To validate the reliability of the model when trained and tested using the new dataset, recognition accuracies were compared using the same model trained and tested using all datasets. The proposed dataset resulted in considerably better performance, achieving 89% recognition accuracy: 14% better than the others. There is plenty of room for improvement, such as by increasing the recognition accuracy to higher than 89%. Additionally, the Shimmer-brand accelerometer could be replaced with a camera for real-time visual HAR.

CONFLICT OF INTEREST STATEMENT

The authors declare that there are no conflicts of interest.

ORCID

Shoba Sivapatham https://orcid.org/0000-0002-4083-2181

REFERENCES

1. P. Casale, O. Pujol, and P. Radeva, *Personalization and user verification in wearable systems using biometric walking patterns*, Personal Ubiquitous Comput. **16** (2012), no. 5, 563–580.
2. S. Sivapatham, R. Ramadoss, A. Kar, and B. Majhi, *Monaural speech separation using GA-DNN integration scheme*, Appl. Acoust. **160** (2020), 107140.
3. D. Ravi, C. Wong, B. Lo, and G.-Z. Yang, *A deep learning approach to on-node sensor data analytics for mobile or wearable devices*, IEEE J. Biomed. Health Inform. **21** (2016), no. 1, 56–64.
4. Q. Zhu, Z. Chen, and Y. C. Soh, *A novel semisupervised deep learning method for human activity recognition*, IEEE Trans. Industr. Inform. **15** (2018), no. 7, 3821–3830.
5. R. Zhu, Z. Xiao, Y. Li, M. Yang, Y. Tan, L. Zhou, S. Lin, and H. Wen, *Efficient human activity recognition solving the confusing activities via deep ensemble learning*, IEEE Access **7** (2019), 75490–75499.
6. M.-O. Mario, *Human activity recognition based on single sensor square HV acceleration images and convolutional neural networks*, IEEE Sensors J. **19** (2018), no. 4, 1487–1498.
7. W. Sousa Lima, E. Souto, K. El-Khatib, R. Jalali, and J. Gama, *Human activity recognition using inertial sensors in a smartphone: An overview*, Sensors **19** (2019), no. 14, 3213.
8. T. Hur, J. Bang, T. Huynh-The, J. Lee, J.-I. Kim, and S. Lee, *Iss2Image: A novel signal-encoding technique for CNN-based human activity recognition*, Sensors **18** (2018), no. 11, 3910.
9. H. Amroun, M. H. H. Temkit, and M. Ammi, *Best feature for CNN classification of human activity using IoT network*, (IEEE International Conference on Internet of Things (iThings) and IEEE Green Computing and Communications (GreenCom) and IEEE Cyber, Physical and Social Computing (CPSCom) and IEEE Smart Data (SmartData), Exeter, UK), 2017, pp. 943–950.
10. R. Zhu, Z. Xiao, M. Cheng, L. Zhou, B. Yan, S. Lin, and H. Wen, *Deep ensemble learning for human activity recognition using smartphone*, (IEEE 23rd International Conference on Digital Signal Processing (DSP), Shanghai, China), 2018, pp. 1–5.
11. M. Alessandrini, G. Biagetti, P. Crippa, L. Falaschetti, and C. Turchetti, *Recurrent neural network for human activity*

recognition in embedded systems using PPG and accelerometer data*, Electronics **10** (2021), no. 14, 1715.

12. L. Falaschetti, G. Biagetti, P. Crippa, M. Alessandrini, D. F. Giacomo, and C. Turchetti, *A lightweight and accurate RNN in wearable embedded systems for human activity recognition*, *Intelligent decision technologies*, Springer, 2022, pp. 459–468.
13. A. Bensalah, J. Chen, A. Fornés, C. Carmona-Duarte, J. Lladós, and M. A. Ferrer, *Towards stroke patients' upper-limb automatic motor assessment using smartwatches*, (Pattern recognition. ICPR International Workshops and Challenges, Virtual Event), 2021, pp. 476–489.
14. H. E. M. Braakhuis, J. B. J. Bussmann, G. M. Ribbers, and M. A. M. Berger, *Wearable activity monitoring in day-to-day stroke care: a promising tool but not widely used*, Sensors **21** (2021), no. 12, 4066.
15. B. Bruno, F. Mastrogiovanni, and A. Sgorbissa, *A public domain dataset for ADL recognition using wrist-placed accelerometers*, (The 23rd IEEE International Symposium on Robot and Human Interactive Communication, Edinburgh, UK), 2014, pp. 738–743.
16. E. De-La-Hoz-Franco, P. Ariza-Colpas, J. M. Quero, and M. Espinilla, *Sensor-based datasets for human activity recognition–a systematic review of literature*, IEEE Access **6** (2018), 59192–59210.
17. S. Sivapatham, A. Kar, and R. Ramadoss, *Performance analysis of various training targets for improving speech quality and intelligibility*, Appl. Acoust. **175** (2021), 107817.
18. K. Ashwini, R. Amutha, R. Rajavel, and D. Anusha, *Classification of daily human activities using wearable inertial sensor*, (International Conference on Wireless Communications Signal Processing and Networking (WISPNET), Chennai, India), 2020, pp. 1–6.
19. N. A. Capela, E. D. Lemaire, and N. Baddour, *Feature selection for wearable smartphone-based human activity recognition with able bodied, elderly, and stroke patients*, PloS One **10** (2015), no. 4, e0124414.
20. M. K. O'Brien, N. Shawen, C. K. Mummidisetty, S. Kaur, X. Bo, C. Poellabauer, K. Kording, and A. Jayaraman, *Activity recognition for persons with stroke using mobile phone technology: Toward improved performance in a home setting*, J. Med. Int. Res. **19** (2017), no. 5, e7385.
21. D. Garcia-Gonzalez, D. Rivero, E. Fernandez-Blanco, and M. R. Luaces, *A public domain dataset for real-life human activity recognition using smartphone sensors*, Sensors **20** (2020), no. 8, 2200.
22. M. Ahmed, N. Mehmood, A. Nadeem, A. Mehmood, and K. Rizwan, *Fall detection system for the elderly based on the classification of shimmer sensor prototype data*, Healthcare Inform. Res. **23** (2017), no. 3, 147–158.
23. L. Venkataramana, S. G. Jacob, R. Ramadoss, D. Saisuma, D. Haritha, and K. Manoja, *Improving classification accuracy of cancer types using parallel hybrid feature selection on microarray gene expression data*, Genes Genomics **41** (2019), no. 11, 1301–1313.
24. S. Ashry, R. Elbasiony, and W. Gomaa, *An LSTM-based descriptor for human activities recognition using IMU sensors*, (Proceedings of the 15th International Conference on Informatics in Control, Automation and Robotics, ICINCO, Vol. **1**, Porto, Portugal), 2018, pp. 494–501.

AUTHOR BIOGRAPHIES

Anusha David completed her postgraduate study in the Department of Electronics and Communication Engineering at the SSN College of Engineering, Chennai, India. She completed her ME of applied electronics degree at SSN College from 2018 to 2020.

Rajavel Ramadoss is an associate professor in the Department of Electronics and Communication Engineering at the SSN College of Engineering, Chennai, India. He has 20 years' experience with 4 years of research, 1 year in industry, and 15 years of teaching. He has published more than 50 research papers in refereed international journals and proceedings at national and international conferences. He is a recognized supervisor at Anna University in Chennai, India, having supervised two PhD graduates. Presently, he is supervising five PhD students in speech signal processing, audio–visual speech enhancement, and rotating machine fault diagnosis. His areas of interest include signal and speech processing, machine learning, and deep learning.

Amutha Ramachandran is a professor in the ECE department, having graduated from the Thiagarajar College of Engineering, India, in 1987. She obtained her ME degree from the PSG College of Technology and her PhD from Anna University, India, in 2006. She has 35 years of teaching experience and 20 years research. Her research areas include wireless communication networks, signal processing, and image processing. She has published 40 international and four national journal papers and has at least 100 international and national conference papers to her credit. She completed two projects (i.e., ambient-assisted living and energy-efficient image communications over wireless sensor networks) as a principal investigator funded by SSN Trust. She currently manages the "Design of Game-Based Communication Platform for Children with Cerebral Palsy," which is funded by DST. She is a reviewer for the IEEE Journal of Electronic Imaging, ETRI, and Elsevier International Journals. She is a recognized research supervisor at Anna University for PhD and MS research. Twelve PhD scholars have graduated under her guidance, and she is presently guiding three PhD research scholars.

Shoba Sivapatham received a post-doctorate fellowship at IIITDM Kancheepuram and a PhD from Anna University, India. She is employed as an assistant professor at the Center for Advanced Data Science at the Vellore Institute of Technology, Chennai, India. She has published approximately 20 papers in peer-reviewed international journals and conferences. She is a technical reviewer for top-quality Elsevier, Springer, and IET journals. Her research interests include speech signal processing, deep learning, computer vision, and natural language processing. Examples of more specific research interests within this scope include enhancement, separation, modeling, and analysis. Furthermore, she is a member of IEEE and ISTE.

How to cite this article: A. David, R. Ramadoss, A. Ramachandran, and S. Sivapatham, *Activity recognition of stroke-affected people using wearable sensor*, ETRI Journal **45** (2023), 1079–1089. https://doi.org/10.4218/etrij.2022-0242